# Resonance Raman Examination of the Wavelength Regulation Mechanism in Human Visual Pigments†

Gerd G. Kochendoerfer,‡ Zhiyan Wang,§ Daniel D. Oprian,§ and Richard A. Mathies*,‡

*Department of Chemistry, University of California, Berkeley, California 94720, and Department of Biochemistry, Brandeis University, Waltham, Massachusetts 02254*

*Received February 12, 1997; Revised Manuscript Received March 27, 1997*⊗

ABSTRACT: Resonance Raman spectra of recombinant human green and red cone pigments have been obtained to examine the molecular mechanism of color recognition by visual pigments. Spectra were acquired using a 77 K resonance Raman microprobe or preresonance Raman spectroscopy. The vibrational bands were assigned by comparison to the spectra of bovine rhodopsin and model compounds. The C═NH stretching frequencies of rhodopsin, the green cone pigment, and the red cone pigment in $H_2O$ ($D_2O$) are found at 1656 (1623), 1640 (1618), and 1644 $cm^{-1}$, respectively. Together with previous resonance Raman studies on iodopsin [Lin, S. W., Imamoto, Y., Fukada, Y., Shichida, Y., Yoshizawa, T., & Mathies, R. A. (1994) *Biochemistry 33*, 2151−2160], these values suggest that red and green pigments have very similar Schiff base environments, while the Schiff base group in rhodopsin is more strongly hydrogen-bonded to its protein environment. The absence of significant frequency and intensity differences of modes in the fingerprint and the hydrogen out-of-plane wagging regions for all these pigments does not support the hypothesis that local chromophore interactions with charged protein residues and/or chromophore planarization are crucial for the absorption differences among these pigments. However, our data are consistent with the idea that the Schiff base group in blue visual pigments is stabilized by protein and water dipoles and that the removal of this dipolar field shifts the absorption maximum from blue to green. A further red shift of the $\lambda_{max}$ from the green to the red pigment is successfully modeled by the addition of hydroxyl-bearing amino acids ($Ser_{164}$, $Tyr_{261}$, and $Thr_{269}$) close to the ionone ring that lower the transition energy by interacting with the change of dipole moment of the chromophore upon excitation. The increased hydrogen bonding of the protonated Schiff base group in rhodopsin is predicted to account for the 30 nm blue shift of its absorption maximum compared to that of the green pigment.

Human color vision is initiated by a set of three photoreceptors found in three distinct types of cone cells in the retina. Their wavelengths of maximal absorbance are 410 nm (blue cone), 530 nm (green cone), and 560 nm (red cone; Merbs & Nathans, 1992; Oprian et al., 1991). Rhodopsin, the visual pigment that drives scotopic (dim-light) vision, absorbs maximally at 500 nm (Wald & Brown, 1954). All of these visual pigments are integral membrane proteins belonging to the family of seven-α-helix G-protein-coupled receptors. The light-absorbing species in each pigment is an 11-*cis*-retinal chromophore that is attached to the protein via a protonated Schiff base linkage to a conserved lysine residue. The difference of the absorption maximum of the 11-*cis*-retinal-protonated Schiff base chromophore in organic solvents compared to that of the protein-bound form has been termed the opsin shift (Nakanishi et al., 1980). While a great deal of effort has been devoted to investigating the mechanism by which the protein regulates the absorption maximum of the visual chromophore, the physical mechanism of the opsin shift is not understood.

The amino acid sequences for a large number of vertebrate and invertebrate visual pigments are now known (Hargrave et al., 1983; Nathans et al., 1986; Okano et al., 1992; Ovchinnikov et al., 1982; Yokoyama & Yokoyama, 1990). Vertebrate pigments can be separated by sequence homology into four groups according to their absorption maxima at short (group S), medium (groups $M_1$ and $M_2$), or long (group L) wavelengths (Okano et al., 1992). Blue-absorbing pigments belong to either group S or $M_1$. Examples are the human blue cone pigment which belongs to group S and the chicken blue pigment which belongs to group $M_1$. Green-absorbing pigments, such as rhodopsin or the chicken green pigment, belong to group $M_2$. Most other green and red cone receptors, such as the human green and red cone pigments, belong to group L. The high sequence similarity among receptors within each group suggests that there are common physical mechanisms that determine the absorption maximum in each pigment group.

On the basis of retinal analog studies, calculations, and sequence comparison, several chromophore-protein interactions have been postulated to regulate the opsin shift. These involve (1) a weakening of the interaction of the positive charge of the retinal-protonated Schiff base with its negative counterion or hydrogen-bonding partner (Baasov et al., 1987; Blatz et al., 1972); (2) The placement of full or partial charges (Asenjo et al., 1994; Beppu & Kakitani, 1994; Honig et al., 1976; Kropf & Hubbard, 1958; Neitz et al., 1991) or polarizable groups (Blatz & Mohler, 1975; Irving et al., 1970) close to the polyene chain; and (3) Planarization of the polyene chain caused by the protein environment (Blatz & Liebman, 1973). In addition, a 6-s *cis*−*trans* single bond isomerization was proposed to account for part of the red

† This work was supported by NIH Grants EY-02051 (R.A.M.) and EY-09514 (D.D.O.).

* Author to whom correspondence should be addressed.
‡ University of California.
§ Brandeis University.

⊗ Abstract published in *Advance ACS Abstracts,* May 15, 1997.

S0006-2960(97)00322-X CCC: $14.00 

shift in the chicken cone pigment iodopsin (Chen et al., 1989). However, Makino et al. (1990) incorporated 6-s *cis*-locked 11-*cis*-retinal into the opsins of the monkey red and green pigment and observed that the absorption difference between the two analog pigments was identical to the difference between the wild type pigments. This indicated that 6-s *cis*-*trans* isomerization did not cause the absorption difference between these two pigments. To determine which mechanism or mechanisms are playing a role in the opsin shift, one must compare the electronic and structural properties of a variety of different visual pigments.

Raman spectroscopy has been extensively used to investigate chromophore structure and chromophore-protein interactions in rhodopsin and several other rod and cone pigments (Barry & Mathies, 1987; Huang et al., 1996; Lin et al., 1992, 1994; Loppnow et al., 1989; Mathies et al., 1976, 1987; Oseroff & Callender, 1974). Unlike optical absorption, vibrational techniques provide vibrational *structural* information that defines and locates protein-chromophore interactions and therefore can help to determine which of the above mechanisms is responsible for spectral tuning in visual pigments. The first Raman spectra of color visual pigments were obtained from individual, intact receptors of a variety of vertebrate species (Barry & Mathies, 1987). This study suggested that differential charge perturbations of the chromophore do not regulate the absorption maxima of color visual pigments. A more detailed Raman study of the green rod pigment from the toad *Bufo marinus* ($\lambda_{max} = 440$ nm) showed that its chromophore is a protonated retinal Schiff base that is minimally perturbed relative to the chromophore in methanol solution (Loppnow et al., 1989). Lin et al. (1992) developed a confocal Raman microprobe technique that allows for the investigation of microgram quantities of recombinant photosensitive proteins. This technique was later used to obtain Raman spectra of iodopsin, the red-absorbing pigment from the chicken. They concluded that the red shift in this pigment is due to protein interactions in the vicinity of the protonated Schiff base and long-range electrostatic actions (Lin et al., 1994).

The recent synthesis of the genes encoding the three human cone pigments and their overexpression in monkey kidney cells (COS-1)[1] in microgram quantities (Oprian et al., 1991) allow these pigments to be studied for the first time using the Raman microprobe technique. In this paper, we present the first Raman spectra of the human green and red cone pigments. Our data are consistent with the idea that the opsin shift from rhodopsin to the green pigment is determined by the weakening of the interaction of the rhodopsin chromophore with a protein hydrogen bond donor (such as a water molecule) adjacent to the protonated Schiff base group. A further red shift in the red cone pigment is achieved by the interaction of the chromophore with several hydroxyl-bearing amino acids near the ionone ring that couple with the chromophore's electrostatic dipole and differentially stabilize the excited state. A molecular model that illustrates the molecular mechanisms responsible for the absorption maxima in all four human visual pigments is presented.

[1] Abbreviations: COS, cone outer segment; HEPES, *N*-(2-hydroxyethyl)piperazine-*N*′-2-ethanesulfonic acid; PC, phosphatidylcholine; CCD, charge-coupled device; CVFF, consistent valence force field; CHAPS, 3-[(3-cholamidopropyl)dimethylammonio]-1-propanesulfonate; PSB, protonated Schiff base; PMSF, phenylmethanesulfonyl fluoride; HOOP, hydrogen out-of-plane; TFE, trifluoroethanol; HFIP, hexafluoro-2-propanol.

## MATERIALS AND METHODS

*Preparation of Human Color Pigments*. The synthesis of the genes encoding human color visual pigments and their expression, regeneration, and purification was previously described (Oprian et al., 1991). Briefly, COS cells were transfected with the opsin genes and harvested ~72 h after transfection. The synthesized opsin was reconstituted with 11-*cis*-retinal, solubilized in buffer A [50 mM HEPES, 140 mM NaCl, 0.75% (w/v) CHAPS, 0.8 mg/mL PC, 1 mM $CaCl_2$, 1 mM $MnCl_2$, 1 mM PMSF at pH 6.5], and purified by an immunoaffinity procedure using a rhodopsin-like epitope tag and anti-rhodopsin monoclonal antibodies (Oprian et al., 1987). A typical sample required transfection of ~100 plates, yielding ~100 $\mu$g of purified cone pigment. The samples were concentrated to a final volume of 50 $\mu$L having an optical density of 1.5 OD/cm for the green pigment and 0.5 OD/cm for the red pigment. The green pigment was deuterated by dialysis of a part of the sample into deuterated buffer A using a QuickSep Microdialyzer (Membrane Filtration Products, Inc., San Antonio, TX).

*Preresonance Raman Scattering*. Raman excitation was performed by spherically focusing a 30 mW, 795 nm beam from a Lexel 479 Ti:Sapphire laser pumped by the all-lines output from an $Ar^+$ laser (Spectra-Physics 2020) onto ~3 $\mu$L of pigment solution in a 300 $\mu$m inside diameter circular capillary. Nitrogen gas cooled to ~0 °C in a 2-propanol/$CO_2$ bath was blown over the sample to prevent thermal degradation. No significant sample bleaching due to thermal or photochemical processes was observed during the experiment. Scattered light was detected at 90° by a CCD detector (LN/CCD 1152, Princeton Instruments) coupled to a Spex 1401 double spectrograph. Frequencies were calibrated by comparison with the Raman spectrum of cyclohexanone and a Ne lamp emission spectrum. Reported frequencies are accurate to $\pm 2$ cm$^{-1}$, and the spectral resolution is 6 cm$^{-1}$.

*Confocal Resonance Raman Spectroscopy*. The Raman microprobe apparatus used to obtain the low-temperature Raman spectra was previously described (Lin et al., 1992, 1994; Loppnow & Mathies, 1989). Briefly, coaxial beams of 568 nm probe light from a $Kr^+$ laser (Spectra Physics 2025) and 750 nm pump light from the Ti:Sapphire laser were focused by a 40× high-NA objective onto an ~60 × 8 $\mu$m area of the sample. For experiments on the red pigment, the probe wavelength was 585 nm from a rhodamine 6G dye laser (Coherent 465) and the pump wavelength was 676.6 nm from the $Kr^+$ laser.

Approximately 2 $\mu$L of pigment solution and 2 $\mu$l of a bleached control were placed in adjacent microcells on a cold stage (Lin et al., 1992; Loppnow & Mathies, 1989) and frozen at 77 K. Backscattered light was detected confocally with a LN-cooled CCD detector (LN/CCD1152, Princeton instruments) coupled to a Spex 1401 spectrograph. Flat-field correction was achieved by exciting a rhodamine 6G solution in ethylene glycol in the experimental geometry and correcting this experimental spectrum with the absolute fluorescence spectrum of rhodamine 6G obtained on a Perkin-Elmer PMF 44B fluorimeter. Frequencies were calibrated as described above.

*Computational Methods*. A structural model of rhodopsin was built using Insight, and the protein structure was minimized using Discover. Minimization was performed

using the CVF force field. The force field parameters for the chromophore polyene chain were modified to account for its conjugated nature. The necessary modifications were a reduction (increase) of the standard single (double) bond length and an increase (reduction) of the single (double) bond stretching and torsional force constants. The parameters were optimized to reproduce the crystal structure of 11-*cis*-retinal (Drikos et al., 1981). The modified force field parameters are given in Table 1 of the Supporting Information. To model the cone pigment structures, the residues thought to be important for wavelength tuning were replaced with the respective cone pigment residues and the structure was minimized to remove local perturbations.

INDO-CI calculations were performed using a program provided by R. R. Birge of Syracuse University (Hubbard, 1981; Tallent et al., 1992). The retinal chromophore in rhodopsin was represented by the *N*-ethyl-protonated Schiff base of 11-*cis*-retinal. We employed a previously established cutoff procedure (Hubbard, 1981) to determine the number of single and double excitations from a total of 150 single and 290 double excitations included in the configuration interaction calculation. Typically, ~30 single and ~60 double excitations were included. The charge distribution was calculated by a Mulliken analysis of the total electronic wave function. The $Glu_{113}$ counterion in rhodopsin and in the cone pigments (cone pigment residues are identified with the sequence number of the homologous rhodopsin residue throughout the paper) was represented by a carboxyl group. Water that was hydrogen-bonded to the protonated Schiff base group was represented by point charges of −0.82 and 0.41 for oxygen and hydrogen, respectively. The hydroxyl dipoles of environmental amino acids were represented by point charges of −0.38 and 0.35 for oxygen and hydrogen, respectively. The orientation of the dipoles that best fit the experimental mutant absorption data was introduced into the molecular model. The coordinates of the minimized retinal PSB molecule, the adjacent water molecule, the carboxylate counterion, and the hydroxy dipoles used in the INDO-CI calculation are presented in Table 2 of the Supporting Information. Figure 9 of the Supporting Information presents the minimized geometry of the 11-*cis*-retinal chromophore and its PSB terminus with water molecules 1.8 and 3 Å from the PSB proton.

## RESULTS

Preresonance Raman spectroscopy is a useful technique for the structural examination of small amounts of photosensitive pigments. The choice of red excitation wavelengths prevents photochemical bleaching of the sample, thereby avoiding sample degradation and scattering from photochemical intermediates. The technique requires very small sample volumes (3 $\mu$L) and is insensitive to typical fluorescent impurities. The use of an excitation wavelength just outside the pigment absorption band still allows for strong preresonance enhancement of chromophore Raman bands relative to protein, buffer, and bleached pigment bands. This can be appreciated by comparing our spectra to results from 1064 nm-excited FT-Raman experiments, in which the Raman intensity from the bleached products is the same order of magnitude as the pigment intensity (Sawatzki et al., 1990).

*Raman Spectroscopy*. Figure 1 presents the preresonance Raman spectrum of a 1.5 OD/cm solution of the human green pigment, the spectrum of the same solution after bleaching,

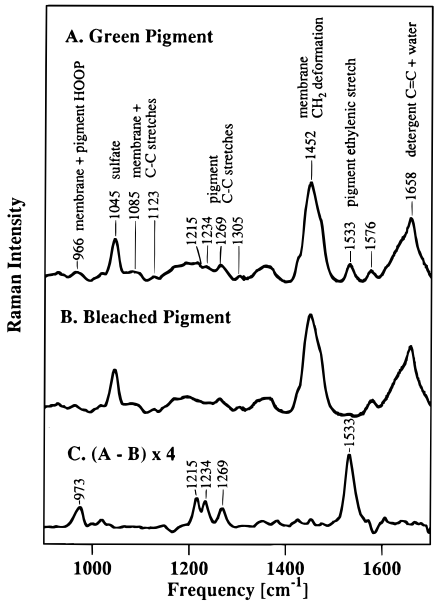


FIGURE 1: (A) Room-temperature preresonance Raman spectrum of the human green cone pigment in $H_2O$ buffer excited with 30 mW at 795 nm, (B) its bleached solution, and (C) the difference spectrum between these spectra, multiplied by a factor of 4.

and their difference spectrum. Despite the use of excitation outside the absorption band of the green pigment chromophore and the almost 3 orders of magnitude lower concentration of pigment compared to that of buffer and detergent, the preresonance Raman enhancement of the chromophore Raman bands allows for their identification in the raw spectrum (Figure 1A). The most prominent chromophore Raman band is the ethylenic stretch at 1533 $cm^{-1}$. Further weak chromophore bands are present around 1250 and 970 $cm^{-1}$. We observed little change in intensity of the chromophore Raman bands during the spectral acquisition time of ~2 h, suggesting that excitation occurs sufficiently outside the absorption band to ensure the absence of photochemical bleaching. The overall spectrum is dominated by bands originating from the CHAPS/PC/HEPES buffer system. The largest band at 1452 $cm^{-1}$ is assigned to alkyl $CH_2$ deformations. Further peaks attributed to the buffer and detergent are the PC C═C stretches at 1658 $cm^{-1}$, several C−C stretches between 1000 and 1200 $cm^{-1}$, and HOOP vibrations around 970 $cm^{-1}$ (Mendelsohn, 1972). The peak at 1045 $cm^{-1}$ is attributed to stretching vibrations of sulfate groups of HEPES and CHAPS. The intense and broad water bending band is centered at ~1640 $cm^{-1}$. After bleaching of the pigment with white light, the chromophore contributions to the spectrum are largely eliminated as the chromophore absorption maximum shifts to 380 nm, causing a large reduction in the preresonance enhancement of its bands. There appears to be very little change in the membrane and detergent bands in the bleached spectrum (Figure 1B), allowing subtraction of the blank without producing artifacts.

The difference spectrum between the bleached and the unbleached sample is presented in Figure 1C and more clearly in Figure 2B. This difference spectrum displays exclusively bands assignable to the 11-*cis*-retinal chromophore. The frequencies in this spectrum are very similar to those in the spectrum of bovine rhodopsin displayed in Figure 2A (Mathies et al., 1987; Palings et al., 1987). This makes it highly likely that these vibrational bands have a normal mode character that is similar to the rhodopsin bands that have been assigned in studies with isotopically labeled

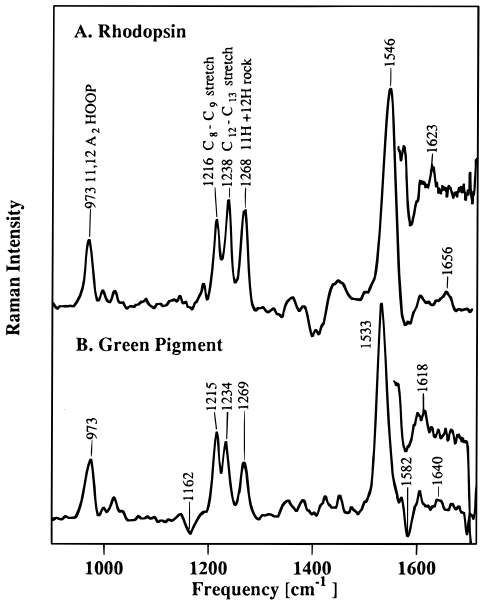


FIGURE 2: Room-temperature preresonance Raman spectrum of bovine rhodopsin (A) and the human green cone pigment (B) in $H_2O$ buffer excited with 30 mW at 795 nm. The insets present the Schiff base regions of the respective spectra obtained from samples in $D_2O$ buffer under the same conditions.

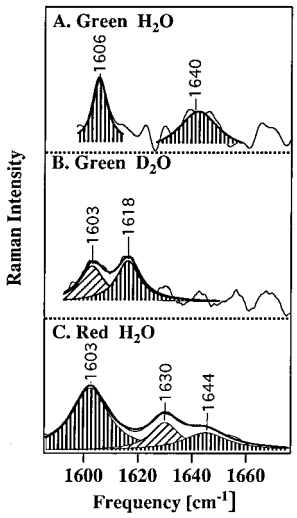


FIGURE 3: Comparison of the C═N stretching region of the room-temperature preresonance Raman spectra of the green pigment in $H_2O$ (A) and $D_2O$ buffer (B) and the 77 K resonance Raman spectrum of the red pigment in $H_2O$ buffer (C). Each band was fit with a Lorentzian line shape function. The Lorentzian band widths (FWHM) were 19 and 12 cm$^{-1}$ for the green pigment in $H_2O$ and $D_2O$ buffer, respectively, and 23 cm$^{-1}$ for the red pigment.

chromophores and retinal analogs (Mathies et al., 1987). On the basis of this comparison, the band at 1640 cm$^{-1}$ in the green pigment is assigned to the C═N stretching vibration coupled to N−H bending motion. Figure 3A presents an expanded view of the Schiff base stretching region of the green pigment in $H_2O$ buffer and a Lorentzian band shape fit of the 1640 cm$^{-1}$ band. Upon dialysis into $D_2O$, this band narrows and shifts down to 1618 cm$^{-1}$ as demonstrated in the inset in Figure 2B and the Lorentzian band shape fit in Figure 3B. The band at 1533 cm$^{-1}$ in Figure 2B is assigned to a combination of ethylenic double bond stretches. The bands at 1215, 1234, and 1269 cm$^{-1}$ are assigned to the $C_8$−$C_9$ and $C_{12}$−$C_{13}$ single bond stretches and the 11H + 12H $A_u$ rocking mode, respectively. The band at 973 cm$^{-1}$ is assigned to the 11,12 $A_2$ HOOP mode. The negative bands

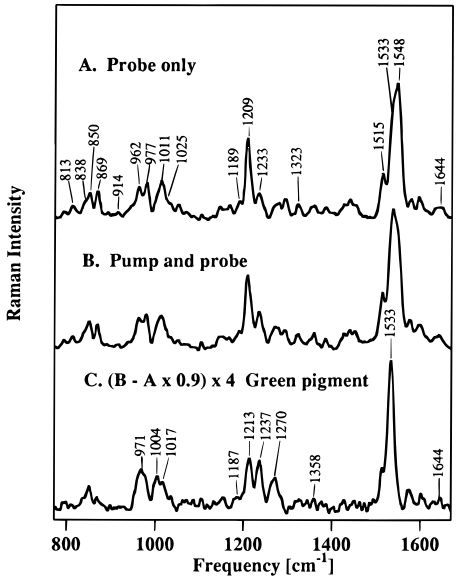


FIGURE 4: Resonance Raman microprobe spectra of the human green cone pigment in $H_2O$ buffer at 77 K obtained (A) with 4 mW of 568 nm probe excitation and (B) with 4 mW of 568 nm probe excitation and 10 mW of 720 nm pump excitation. (C) Spectrum of the green pigment calculated from the difference of the spectra of parts A and B.

at 1162 and 1582 cm$^{-1}$ most likely originate from subtraction of scattering from the pigment bleaching product.

Raman spectra were also obtained from a photostationary mixture of the green pigment, its iso (9-*cis*) form, and its batho (*all-trans*) form. Figure 4 presents Raman spectra of the human green pigment at 77 K with 568 nm excitation. The ethylenic region exhibits three major bands, suggesting the establishment of a photostationary mixture among the 11-*cis*, 9-*cis*, and *all-trans* species in analogy to rhodopsin (Oseroff & Callender, 1974). The presence of the *all-trans* species is supported by the observation of characteristic HOOP intensity at 813, 838, 850, 869, and 914 cm$^{-1}$ and the low-frequency 1515 cm$^{-1}$ ethylenic band (Eyring et al., 1982). These HOOP bands are at almost the same frequencies as the HOOP bands observed in the photostationary state formed by iodopsin and can therefore be assigned by correspondence (Lin et al., 1994). The band at 813 cm$^{-1}$ is assigned to the $HC_7$═$C_8H$ $B_g$ HOOP. The shoulder at 838 cm$^{-1}$ and the band 850 cm$^{-1}$ are assigned to the $C_{12}$−H wag and the $C_{14}$−H wag, respectively. The bands at 869 and 914 cm$^{-1}$ are assigned to the $C_{10}$−H and $C_{11}$−H wags, respectively. The presence of the 9-*cis* species is supported by the observation of a band at 1323 cm$^{-1}$ that is a marker band for 9-*cis*-retinals, the HOOP intensity at 962 cm$^{-1}$, and a blue-shifted ethylenic band at 1548 cm$^{-1}$ (Curry, 1983). Addition of a pump beam at 700 nm alters the composition of the photostationary state, mainly by affecting the intensity ratio between the bands at 1533 and 1548 cm$^{-1}$ as shown in Figure 4B. Subtraction of the probe-only spectrum from the spectrum in the presence of the pump beam yields the difference spectrum displayed in Figure 4C. While this spectrum exhibits a small contribution from the batho species (as shown by the residual intensity at 1515 cm$^{-1}$), it is largely dominated by the 11-*cis* species. The main peaks in the ethylenic region, the fingerprint region, and the HOOP region have frequencies and intensities that are very similar to those in the preresonance Raman spectrum of the green pigment. However, there is a 4 cm$^{-1}$ upshift of the C═N stretching frequency to 1644 cm$^{-1}$ compared to the room-temperature

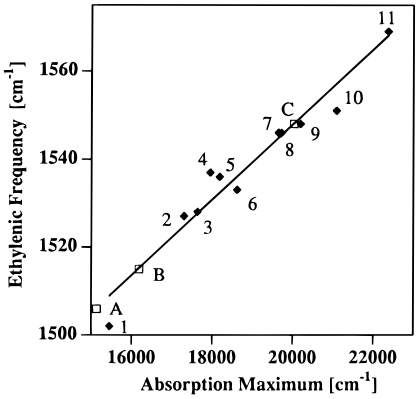


FIGURE 5: Correlation of the ethylenic frequencies of vertebrate visual pigments with their absorption maxima at 77 K. The room-temperature absorption maxima have been corrected for the red shift typically observed upon reduction of the temperature to 77 K by adding 7 nm to the room-temperature absorption maximum (Yoshizawa, 1972). The pigments and their respective absorption maxima and ethylenic frequencies at 77 K (◆) are (1) bathoiodopsin (640 nm, 1502 cm$^{-1}$; Lin et al., 1994), (2) iodopsin (571 nm, 1527 cm$^{-1}$; Lin et al., 1994), (3) human red cone (567 nm, 1528 cm$^{-1}$), (4) isoiodopsin (550 nm, 1527 cm$^{-1}$; Lin et al., 1994), (5) bathorhodopsin (543 nm, 1536 cm$^{-1}$; Eyring et al., 1982), (6) human green cone (537 nm, 1533 cm$^{-1}$), (7) toad red rod (509 nm, 1547 cm$^{-1}$; Barry & Mathies, 1987), (8) rhodopsin (507 nm, 1546 cm$^{-1}$), (9) isorhodopsin (495 nm, 1548 cm$^{-1}$; Palings et al., 1987), (10) gecko rod (474 nm, 1551 cm$^{-1}$; Barry & Mathies, 1987), and (11) toad rod (447 nm, 1569 cm$^{-1}$; Loppnow et al., 1989). The open squares correlate our experimental ethylenic frequencies for the photoproducts of the human cone pigments to their respective absorption maxima. A represents the batho form of the red pigment, and B and C represent the batho and iso forms of the green pigment, respectively.

value. This frequency shift was reproduced within ±1 cm$^{-1}$ in three independent experiments. Due to the higher fluorescence background of pigment samples in $D_2O$, 77 K Raman microprobe spectra of the human cone pigment samples in $D_2O$ with a sufficient signal-to-noise ratio could not be obtained.

The correlation between the absorption maximum and the ethylenic frequency can be used to estimate the absorption maxima of the pigments in the photostationary state. The calibration curve presented in Figure 5 is established by linear regression analysis of ethylenic frequencies and absorption maxima of a variety of visual pigments studied previously. This analysis suggests absorption maxima of ∼625 nm for the batho form and ∼492 nm for the iso form of the human green cone pigment.[2] The 1533 cm$^{-1}$ frequency for the green pigment corresponds to an absorption maximum of 548 nm, close to the expected value of ∼537 nm.

Figure 6A presents the 77 K Raman microprobe spectrum of the human red pigment excited at 585 nm. The presence of several ethylenic bands suggests the establishment of a photostationary state. The spectrum of the human red pigment is almost identical to that of iodopsin (Lin et al., 1994) and is therefore assigned by comparison to this pigment. The three isomeric species in this spectrum can be identified in the same manner used for the green pigment.

[2] The deduced absorption maximum for the 9-*cis* species of the green pigment (492 nm) is unusually blue-shifted relative to the absorption maximum of the 11-*cis* species. This observation is not without precedent. The absorption maximum of the 9-*cis* form of the green pigment at room temperature is at 504 nm (S. L. Pelletier and D. D. Oprian, unpublished results). Furthermore, low-temperature absorption studies on gecko green photoreceptors show that this pigment ($\lambda_{max}$ = 522 nm) forms a 9-*cis* species that absorbs at 488 nm (Crescitelli, 1982).

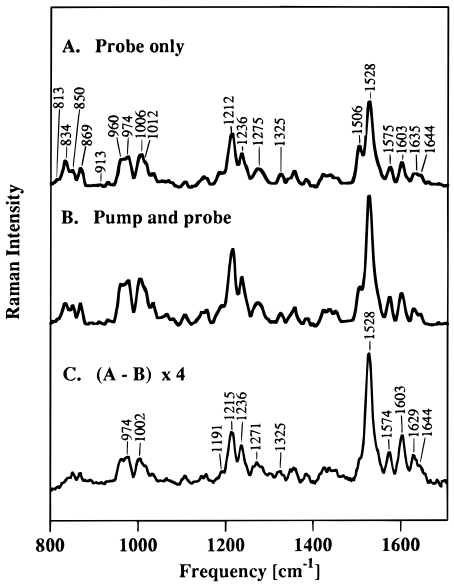


FIGURE 6: (A) Resonance Raman microprobe spectra of the human red cone pigment in $H_2O$ buffer at 77 K obtained (A) with ∼2.5 mW of 585 nm probe excitation and (B) with ∼2.5 mW of 585 nm probe excitation and 5 mW of 676 nm pump excitation. (C) Spectrum of the red pigment 11-*cis* and 9-*cis* mixture calculated from the difference of the spectra of parts A and B. The spectra were subtracted to minimize the intensity of the HOOP modes around 850 cm$^{-1}$ while avoiding negative bands.

The presence of the *all-trans* species in the photostationary state is supported by the observation of the characteristic strong HOOP modes at 813, 834, 850, 869, and 913 cm$^{-1}$ and a low-energy 1506 cm$^{-1}$ ethylenic band (Eyring et al., 1982). The HOOP modes are at nearly the same frequencies as those of iodopsin (Lin et al., 1994) and are therefore assigned similarly. The band at 813 cm$^{-1}$ is assigned to the $HC_7{=}C_8H$ $B_g$ HOOP. The band at 834 cm$^{-1}$ and the shoulder at 850 cm$^{-1}$ are assigned to the $C_{12}{-}H$ wag and the $C_{14}{-}H$ wag, respectively. The bands at 869 and 914 cm$^{-1}$ are assigned to the $C_{10}{-}H$ and $C_{11}{-}H$ wags, respectively. The ethylenic frequency of 1506 cm$^{-1}$ for the batho species corresponds to an absorption maximum of 640 nm, identical to the value found for bathoiodopsin (Yoshizawa & Wald, 1967). The presence of the 9-*cis* species is supported by the observation of a band at 1325 cm$^{-1}$ that is a marker band for 9-*cis*-retinals, the HOOP intensity at 960 cm$^{-1}$, and a higher-frequency ethylenic band (Curry, 1983). The band at 1528 cm$^{-1}$ is assigned to the ethylenic bands of both the 11-*cis* form and the iso form. The overlap of the 9-*cis* and 11-*cis* ethylenic bands does not allow for the identification of the exact location of the 9-*cis* band. The room-temperature absorption maximum for the iso-form of the red pigment was recently determined to be 521 nm (S. L. Pelletier, and D. D. Oprian, unpublished results). Addition of a pump beam at 676 nm (Figure 6B) significantly reduces the concentration of the batho species as shown by the reduced relative intensity of the 1506 cm$^{-1}$ band. Subtraction of the probe-only spectrum from the pump and probe spectrum yields the difference spectrum displayed in Figure 6C. This spectrum is largely dominated by the 11-*cis* species, but there is a small contribution from peaks assignable to the iso species.

By analogy to iodopsin, the shoulder at 1644 cm$^{-1}$ is assigned to the C═N stretching vibration that is coupled to the N−H rocking vibration. The band at 1528 cm$^{-1}$ is assigned to the ethylenic stretching vibrations, and the bands

at 1215, 1236, and 1271 $cm^{-1}$ are assigned to $C_8-C_9$ stretching, $C_{12}-C_{13}$ stretching, and 11H + 12H $A_u$ rocking vibrations, respectively. The mode at 974 $cm^{-1}$ is assigned to the 11H + 12H $A_2$ HOOP vibration. The shoulder of this band at 960 $cm^{-1}$ is due to the iso species in the difference spectrum. This is supported by the residual intensity at 1326 $cm^{-1}$ that is also characteristic of the iso form.

*INDO-CI Calculations.* Semiempirical INDO-CI calculations were performed to test models for the mechanism of color tuning in visual pigments. We extended the earlier calculations by Han et al. (1993; Han & Smith, 1995) to investigate the influence of the position of dipoles and charges on the absorption maximum. We first calculated the charge distribution and absorption maximum for the *N*-ethyl 11-*cis*-retinal-protonated Schiff base with a $Cl^-$ ion 2.25 Å from the PSB proton (model 1). This corresponds to a likely structure of the retinal PSB with a $Cl^-$ counterion in a nonleveling solvent (Blatz et al., 1972) and in the solid state. The calculated absorption maximum of 430 nm is in good agreement with the experimental value of 440 nm. The calculated charge distribution is reported in Table 2 of the Supporting Information. We then calculated the electron distribution and absorption maximum for the retinal PSB in the absence of any inorganic counterion (model 2) and finally added a carboxylate counterion to model 2 located 3 Å away from the polyene $C_{12}$ in a position similar to the geometry suggested by solid state NMR studies (model 3; Han & Smith, 1995). Finally, a water molecule was added to model 3 with an NH···O distance of 3 Å (model 4). We adopted an optimized water geometry that was the result of recent *ab initio* calculations (Figure 9 of the Supporting Information; Nina et al., 1993, 1995). Removal of the $Cl^-$ counterion (model 2) caused a 6000 $cm^{-1}$ red shift, while addition of the carboxylate counterion (model 3) increased the red shift by 1600 $cm^{-1}$ to 7600 $cm^{-1}$. Addition of a water molecule 3 Å from the Schiff base hydrogen (model 4) resulted in a blue shift of 850 $cm^{-1}$ relative to model 3. The resulting charge distributions for both the ground and the first excited state of model 4 are reported in Table 1 of the Supporting Information.

To test the effect of hydrogen bonding between the PSB and the water molecule on the absorption maximum, we altered their intermolecular distances. Previous *ab initio* calculations predicted the maximum hydrogen bonding strength at a NH···O distance of 1.86 Å and a reduction of hydrogen bonding energy by ~15 and 50% if the distance increased to 2.25 and 3 Å, respectively (Nina et al., 1995). Our calculations predict that the addition of water to the retinal PSB with the carboxylate counterion (model 3) in the ideal hydrogen bonding geometry (1.86 Å) will blue-shift the absorption maximum by ~2000 $cm^{-1}$ relative to model 3.[3] An increase of the water−PSB distance to 2.25 and 3 Å produces smaller blue shifts of 1275 and 850 $cm^{-1}$ relative to model 3, respectively. The shift difference observed between water at full and 50% hydrogen bond strength (i.e. 1.86 and 3 Å distance) is similar to the absorption shift between rhodopsin and the green pigment. In agreement with NMR experiments (Albeck et al., 1992), our calculations demonstrate that a shortened hydrogen bond causes a reduction in electron delocalization due to the proximity of the negatively polarized water oxygen to the retinal PSB terminus.

To investigate the role of hydroxy amino acids in the color-tuning mechanism of red pigments, we performed model calculations in which the three most important hydroxyl-substituted amino acids ($Ser_{164}$, $Tyr_{261}$, and $Thr_{269}$) were introduced into the rhodopsin structure and added to model 4. The coordinates for the hydroxy dipoles are available in Table 2 of the Supporting Information. Addition of the dipoles induced absorption red shifts of 150, 750, and 250 $cm^{-1}$, in satisfactory agreement with the experimental absorption spectral shifts of the corresponding rhodopsin mutants of 75, 400, and 550 $cm^{-1}$, respectively (Chan et al., 1992). No significant alteration in the chromophore charge distribution due to the hydroxy dipoles was observed.

## DISCUSSION

The human eye contains four visual pigments, the blue ($\lambda_{max}$ = 410 nm), green ($\lambda_{max}$ = 530 nm), and red ($\lambda_{max}$ = 560 nm) cone pigments and rhodopsin ($\lambda_{max}$ = 500 nm). The absorption maximum of each pigment is determined by the interaction of the protein environment with the 11-*cis*-retinal chromophore. Raman spectroscopy can clarify the nature of this interaction by identifying spectral differences that are a consequence of local chromophore perturbations. In this report, we present Raman spectra of human visual pigments which permit a direct examination of the mechanism of the opsin shift. The Raman spectra of the red and green human cone pigments will be analyzed by comparison to the vibrational spectra of other visual pigments studied previously, in particular the toad green rod pigment and bovine rhodopsin (Barry & Mathies, 1987; Lin et al., 1994; Loppnow et al., 1989; Mathies et al., 1987). The expected sequence homology and similar absorption properties of the toad "green" rod and the human blue cone pigment (Nathans et al., 1986) and of bovine rhodopsin (Ovchinnikov et al., 1982) and human rhodopsin (94% sequence homology; Nathans & Hogness, 1984) suggest that each pair of proteins has similar protein−chromophore interactions and that the toad green rod pigment and bovine rhodopsin can be used as models for the other two human visual pigments (Nathans et al., 1986; Okano et al., 1992). Our discussion of the mechanism of color tuning is supported by the molecular models of the human blue, green, and red cone pigments presented in Figure 7. The locations of residues believed to be critical for the color-tuning mechanism in these pigments are displayed. The polyene chains are color coded to depict the chromophore electronic property that is most useful in understanding the mechanism that determines the absorption maximum. In combination with the results of INDO-CI calculations and molecular modeling, our vibrational studies provide a mechanistic molecular understanding of the color-tuning mechanism in the four human visual pigments.

*Opsin Shift and Electron Delocalization.* The linear correlation between the visual pigment absorption maxima and their respective ethylenic Raman frequencies, which in turn are a measure of the extent of charge delocalization in the electronic ground state, suggests that the absorption maximum is correlated with the extent of charge delocal-

[3] Our INDO-CI calculation overestimates the opsin shift for rhodopsin by ~2000 $cm^{-1}$. However, in view of the uncertainty of the location of the counterion in the solution structure, the lack of information on the dielectric properties of the protein interior, and the lack of incorporation of additional dipolar groups and water molecules known to be present in the rhodopsin binding pocket, we do not consider this discrepancy to be surprising.

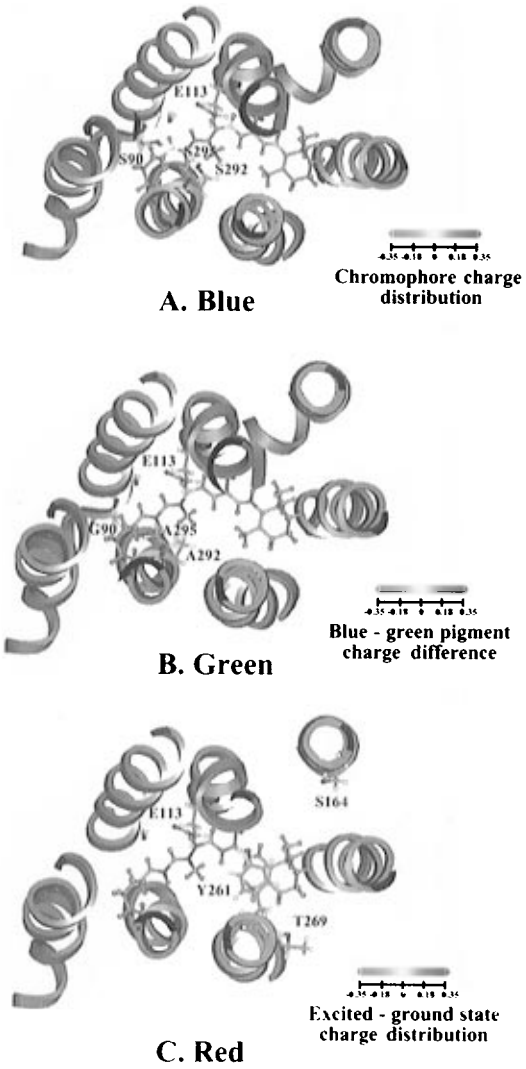


FIGURE 7: Structural model for the retinal binding site in blue (A), green (B), and red (C) visual pigments. The seven α-helices were positioned on the basis of the three-dimensional projection maps of rhodopsins (Davies et al., 1996; Schertler & Hargrave, 1995; Unger & Schertler, 1995), and the faces of the helices were oriented according to the Baldwin model for G-protein-coupled receptors (Baldwin, 1993). The retinal chromophore was oriented to give a counterion−$C_{12}$ distance of 3 Å as deduced from the interpretation of solid-state NMR experiments (Han & Smith, 1995). The ionone ring was placed between helix V and VI on the basis of cross-linking experiments (Nakanishi et al., 1995) and to make possible the interaction of the 3-hydroxy group on the ionone ring with serine residues on helix V as commonly observed in invertebrate rhodopsins (Tanimura et al., 1986). Residues thought to be important for the color tuning in the visual pigments are displayed in standard atom (CPK) colors. The orientation of the hydroxyl groups in the red pigment model was constrained by the INDO-CI calculations of the green−red opsin shift. The polyene color coding in panel A represents the ground state charge distribution in the blue pigment. The polyene color coding in panel B represents the ground state charge distribution difference between the green and blue pigment. The polyene color coding in panel C represents the charge distribution difference between the ground and first excited states in the red pigment.

ization in the chromophore ground state (Aton et al., 1977; Rimai et al., 1970). This correlation is observed for all visual pigments as demonstrated in Figure 5. The ethylenic frequencies drop from 1569 $cm^{-1}$ in the toad green rod ($\lambda_{max}$ = 440 nm) to 1546 $cm^{-1}$ in rhodopsin ($\lambda_{max}$ = 500 nm), 1533 $cm^{-1}$ in the green cone pigment ($\lambda_{max}$ = 530 nm), and 1528 $cm^{-1}$ in the red cone pigment ($\lambda_{max}$ = 560 nm). The correlation between the extent of charge delocalization in the chromophore ground state and the absorption maximum was corroborated in a recent NMR study on retinal analogs by Sheves and co-workers (Albeck et al., 1992). The analysis of the opsin shift in human visual pigments therefore can be approached by understanding the mechanism that causes variation in the ground state electron delocalization along the retinal polyene chain.

Information on charge interactions and hydrogen bonding at the protonated Schiff base group is obtained by observation of the chromophore C═N stretching frequency in $H_2O$ and $D_2O$. The frequency shift of the C═N stretching band upon deuteration of the Schiff base nitrogen depends upon the strength of its hydrogen bond with a solvent molecule, while the frequency of the C═N stretching band in $D_2O$ is a function of electrostatic interactions between the Schiff base and its counterion that affect the C═N bond order (Baasov et al., 1987; Lin et al., 1994; Smith et al., 1983, 1984). The correlation between the $D_2O$ shift and the hydrogen bonding strength is caused by the coupling of the C═N stretching mode to the N−H rocking mode. Deuteration of the nitrogen reduces this coupling as a result of the decreased N−D rocking frequency. The magnitude of the shift upon deuteration is a measure of the strength of hydrogen bonding, since hydrogen bonding increases the N−H rocking frequency and therefore increases the coupling between the N−H and C═N modes (Baasov et al., 1987; Smith et al., 1983, 1984).

Local charge interactions along the polyene chain are detected by frequency shifts in the fingerprint and HOOP region. One example is bathorhodopsin, in which an unusual coupling pattern between individual hydrogen wags was explained by the electrostatic perturbation of the polyene chain by the counterion (Palings et al., 1989). The intensity of HOOP and torsional modes depends on the nonplanarity of the portion of the polyene chain that is involved in a particular normal mode (Kochendoerfer et al., 1996; Palings et al., 1989). We thus have mechanisms for identifying whether the wavelength-tuning mechanism depends on hydrogen bonding changes, charge perturbations, or torsional distortions.

*Green−Red Opsin Shift.* A comparison between the Raman spectra of the red and green cone pigments reveals very few differences. The most obvious difference between the pigments is the 5 $cm^{-1}$ shift of the ethylenic Raman band due to increased charge delocalization as discussed above. The C═N stretching frequencies of the red (1644 $cm^{-1}$) and green (1644 $cm^{-1}$) cone pigments at 77 K are identical. We were not able to obtain Raman spectra of the red pigment in $D_2O$. However, the Raman spectra of iodopsin and the red cone pigment at 77 K in $H_2O$ are virtually identical (Lin et al., 1994). The pigments have a very high sequence similarity (85%), further suggesting that they are structurally similar (Okano et al., 1992).[4] It is therefore reasonable to assume that they have very similar spectra in $D_2O$. The iodopsin C═N stretching frequency at 77 K in $D_2O$ is 1621 $cm^{-1}$ (Lin et al., 1994). Noting that there is a 4 $cm^{-1}$ decrease in the C═N stretching frequency in the green pigment in $H_2O$ going from 77 K (1644 $cm^{-1}$) to room temperature (1640 $cm^{-1}$), the C═N stretching frequency of

[4] The ethylenic frequencies of the red pigment photoproducts are very similar to those of iodopsin (Lin et al., 1994; Yoshizawa & Wald, 1967). This shows that the protein−chromophore interactions in iodopsin and in the human red pigment are very similar.

the red cone pigment at room temperature in $D_2O$ is predicted to lie at 1617 $cm^{-1}$, which is nearly identical to the value for the green pigment in $D_2O$. The similarity of the C═N stretching frequency in the green and red cone pigment in both $H_2O$ and by inference in $D_2O$ suggests that the Schiff base environment is very similar in the green and red pigments. This is supported by mutant studies of human cone pigments. Replacement of the Schiff base counterion in the E113Q mutant moves the absorption maximum from 530 to 488 nm for the green cone and from 560 to 514 nm for the red cone (J. Rim, A. B. Asenjo, and D. D. Oprian, unpublished results). Both pigments therefore undergo a shift of ~1600 $cm^{-1}$ upon counterion removal, suggesting that they have similar Schiff base−counterion interactions. In addition, both cone pigments have a similar p$K_a$ of 9 (Z. Wang, and D. D. Oprian, unpublished results). The similarity of the Schiff base regions of the red and green cone pigments indicates that protein−chromophore interactions outside the Schiff base environment must be responsible for the difference in charge delocalization between these pigments.

Inspection of the fingerprint and HOOP regions of the Raman spectra of the red and green pigments does not reveal any major frequency differences between the 11-*cis* species of the respective pigments. The absence of intensity changes in the HOOP region of the 11-*cis* species suggests that chromophore planarization is not a significant contributor to the difference in the absorption maximum. The band at 960 $cm^{-1}$ observed in the red pigment spectrum can be assigned to the 9-*cis* species and is not due to additional chromophore distortion (Curry, 1983; Kochendoerfer et al., 1996). We infer from the similarity of the spectra of the two pigments that the absorption shift from the green to the red pigment is not caused by local protein perturbations along the chain.

Although the red and green pigment sequences are 96% identical, several nonpolar residues in the chromophore binding site of the green pigment are converted to hydroxyl-bearing residues in the red pigment (Nathans et al., 1986; Oprian et al., 1991). Neitz et al. (1991) have demonstrated that the replacement of these three amino acids is sufficient to explain the 30 nm shift from the green to the red pigment. This was further supported by the work of Chan et al. (1992), who mutated these three amino acids to hydroxy amino acids in rhodopsin and thereby induced red shifts of 75, 400, and 550 $cm^{-1}$, respectively. Asenjo et al. (1994) later found that, while the previously reported three polar amino acids played the dominant role in shifting the absorption maximum from the green to the red, the conversion of four additional residues was needed to fully reproduce the absorption shift. The approximate additivity of the effects of these individual amino acids makes it likely that the dipolar groups interact directly with the chromophore and do not induce a conformational change of the protein.

The results of our INDO-CI calculation support the idea that electrostatic interactions between the additional dipolar residues and the chromophore in the red pigment are suffcient to explain the green−red opsin shift. This interaction can be pictured as a dipole−dipole interaction between the hydroxy dipoles and the dipole moment difference between the ground and excited state of the retinal chromophore. Figure 7C presents a structural model of the chromophore environment in red pigments. The change in charge distribution between the red pigment ground and excited state is depicted by the color-coded polyene chain carbons. The hydroxy dipoles of $Ser_{164}$, $Tyr_{261}$, and $Thr_{269}$ are oriented to interact favorably with the charge distribution difference of the polyene chain. In our rhodopsin model, all three hydroxy dipoles are in the proximity of the ionone ring. Interestingly, incorporation of 3-dehydro-11-*cis*-retinal into salamander red opsin (i.e. extension of the conjugated chain into the ionone ring part of the chromophore) resulted in a larger opsin shift compared to that of the wild type chromophore (Makino et al., 1990). This is consistent with the idea that the protein dipoles in the vicinity of the ionone ring interact electrostatically with the chromophore. We conclude that these long-range electrostatic interactions determine the absorption maximum difference between the red and green pigment. Due to the highly dipolar nature of the retinal excited state (Mathies & Stryer, 1976), the resulting interaction energy preferentially stabilizes the electronic excited state compared to the electronic ground state. This narrows the energy gap between the two states and leads to the observed red-shifted absorption maximum.

*HOOP Modes and Photoproduct Chromophore Structure*. The low-frequency region of the probe-only spectrum of the green and red pigments exhibits bands at 813, ~835, 850, and 869 $cm^{-1}$ and a small peak at ~913 $cm^{-1}$ due to the batho species. The coupling pattern of the respective wags is a function of local charge perturbation as demonstrated previously for bathorhodopsin (Palings et al., 1989). The absence of any significant changes in this coupling pattern suggests that there is no difference between the interaction of the *all-trans* chromophore with the counterion in the red and green pigments. However, one observes a different intensity distribution of the bands at ~835 and 850 $cm^{-1}$ assigned to the $C_{14}$−H and $C_{12}$−H wags, respectively. HOOP intensity is a reflection of differential distortion between the ground and excited electronic state equilibrium geometry (Eyring et al., 1982). This suggests that the green batho species is more distorted in the vicinity of $C_{12}$, while the red batho species is more distorted in the vicinity of $C_{14}$. This difference in the photoproduct chromophore distortion might contribute to their different thermal relaxation pathways. While red pigments like iodopsin undergo thermal relaxation from bathoiodopsin back to iodopsin at 77 K, green pigments like the gecko green pigment convert solely to the next intermediate (Kojima et al., 1995; Yoshizawa & Wald, 1967).

*Opsin Shift from Rhodopsin to Green Pigments*. The most striking difference between the Raman spectra of rhodopsin (Palings et al., 1987) and the green cone pigment is the difference in frequency reduction of the C═N stretch upon deuterium exchange. In rhodopsin, the C═N stretching frequency drops by ~33 $cm^{-1}$, while the shift of the Schiff base stretching mode in the green pigment is only 22 $cm^{-1}$. The reduced deuterium shift indicates that there is a large decrease in hydrogen bonding in the green pigment compared to that in rhodopsin. The reduced $D_2O$ shift in the green pigment is accompanied by a 5 $cm^{-1}$ decrease in the C═N−D stretching frequency, consistent with decreased hydrogen bonding.

Inspection of the fingerprint and HOOP bands of the 11-*cis* species reveals few spectral differences between rhodopsin and the green pigment that provide indication of local perturbations. There is a slight frequency decrease of the band at 1238 $cm^{-1}$ in rhodopsin to 1234 $cm^{-1}$ in the green pigment. While this mode has its largest contribution from $C_{12}$−$C_{13}$ stretching, it is highly mixed with other stretching

and rocking vibrations. A small 4 $cm^{-1}$ shift may therefore be due to slight changes of mode character or coupling.

There are small differences in the frequencies of the HOOP vibrations of the batho form in the green pigment compared to rhodopsin. Most notably, one observes a downshift of the 850 $cm^{-1}$ $C_{14}$−H wagging band in bathorhodopsin to ∼837 $cm^{-1}$. The overall coupling pattern of the hydrogen wagging vibrations remains constant between the green pigment and rhodopsin. We observe the $C_{14}$−H and $C_{12}$−H wags around 950 $cm^{-1}$, a $C_{10}$−H wag at around 970 $cm^{-1}$, and an isolated $C_{11}$−H wag around 920 $cm^{-1}$. The latter band loses intensity going from bathorhodopsin to the green batho form, suggesting a reduction in distortion in the center of the polyene. The green pigment Raman spectra are in marked contrast to the Raman spectra of rhodopsin mutants devoid of a counterion such as the E113A mutant. In this mutant, one observes a single intense band at 887 $cm^{-1}$, assigned to the $C_{10}$−H wag and another band at 933 $cm^{-1}$, assigned to a combination of the $C_{11}$−H and $C_{12}$−H wags (Lin et al., 1992). An almost identical coupling pattern is observed in the case of octopus rhodopsin, where the $Glu_{113}$ counterion is replaced with a tyrosine (Huang et al., 1996). The small differences in the HOOP vibrations between the batho forms of the green pigment and rhodopsin are therefore not indicative of a major change in interaction between the chromophore and its counterion.

*Role of Hydrogen Bonding in the Opsin Shift.* Several retinal analog studies have investigated the effect of hydrogen bonding of the protonated Schiff base on its absorption maximum. Sheves and co-workers studied the effect of increased hydrogen bonding by transferring retinal PSBs from methanol into fluorinated alcohols such as trifluoroethanol (TFE) and hexafluoro-2-propanol (HFIP). These solvents are expected to improve solvation of the negative PSB counterion with a concomitant decrease in hydrogen bonding to the PSB nitrogen. Their NMR studies demonstrated that transfer of the retinal PSB from methanol into TFE led to an increase in electron delocalization accompanied by a red shift of the absorption maximum from 440 to 467 nm (Albeck et al., 1992). The reduction in hydrogen bonding caused a reduction in the $D_2O$ shift from 23 $cm^{-1}$ in methanol to 18 $cm^{-1}$ in TFE as well as a slight reduction in the C═ND stretching frequency (Baasov et al., 1987). An even larger reduction in hydrogen bonding is expected upon transfer of the retinal PSB from methanol into trifluoroacetic acid/methylene chloride. They observed a further decrease of the $D_2O$ shift to 15 $cm^{-1}$, accompanied by a decrease in the C═ND frequency of 6 $cm^{-1}$ and a red shift of 2500 $cm^{-1}$ (Baasov et al., 1987). In summary, these analog studies suggest that the observed differences between the Raman spectra of the green cone pigment and rhodopsin are consistent with a difference in hydrogen bonding strength.

Our INDO-CI calculation demonstrates that a reduction in hydrogen bonding strength resulting in increased electron delocalization is sufficient to explain the absorption shift from rhodopsin to the green pigment. While our treatment of the hydrogen bond does not account for nonelectrostatic hydrogen bond interactions such as charge transfer and exchange effects (Vanquickenborne, 1991), it does demonstrate that the reduced electron delocalization caused by the interaction of a water dipole with the PSB group is sufficient to explain the absorption shift of retinal Schiff bases. We conclude that the weakening of the hydrogen bonding interaction of the PSB with a water molecule in the green cone pigment causes the 30 nm red shift of its absorption maximum relative to that of rhodopsin.

*Structural Factors Influencing Hydrogen Bonding.* The strong hydrogen bonding of the retinal-protonated Schiff base in rhodopsin has been invoked previously to explain the origin of the high p$K_a$ of rhodopsin (p$K_a$ > 16) and its stability in the presence of $NH_2OH$ (Liang et al., 1994). Recent stopped-flow deuterium exchange experiments showed that water was the hydrogen bonding partner of the protonated Schiff base in rhodopsin (Deng et al., 1994). This was hypothesized previously on the basis of the interpretation of two-photon absorption experiments, solid state NMR experiments, and protein dehydration studies (Birge et al., 1985; Han & Smith, 1995; Rafferty & Shichi, 1981).

Conceivably, the reduced hydrogen bonding strength between the green pigment PSB and a water molecule is caused by an unfavorable relative orientation. This might be a result of the competition between the PSB and other hydrogen bonding partners, such as the $Glu_{113}$ counterion and other water molecules, that have been postulated to form a hydrogen-bonded network connecting the water molecule at the Schiff base terminus with the extracellular solvent (Deng et al., 1994). Several investigators reported a dependence of the absorption maximum of group L pigments on the presence of counterions such as $Cl^-$ (Crescitelli, 1982; Kleinschmidt & Harosi, 1992; Wang et al., 1993). Wang et al. (1993) recently identified two conserved positive amino acid residues ($His_{197}$ and $Lys_{200}$) that are located in the intradiskal loop region adjacent to helix IV as major constituents of the chloride ion binding site in the green and red human pigment. One could speculate that the electrostatic potential of a chloride ion located in this binding site causes a reordering of the water molecules in the hydrogen-bonded network. This restructuring could weaken the hydrogen bond between water and the adjacent PSB and thereby shift the absorption maximum to higher wavelengths (Crescitelli, 1982; Kleinschmidt & Harosi, 1992; Wang et al., 1993). The blue shift of the pigments in the absence of chloride could then be due to a reordering of the water molecules after removal of the electrostatic potential of the chloride ion. This hypothesis is consistent with the 500 nm absorption maximum of a green pigment mutant devoid of the chloride binding site (Wang et al., 1993).

*Color Tuning in the Blue Pigment.* Resonance Raman studies of the toad green rod pigment showed that, in this blue-absorbing pigment (belonging presumably to either the pigment group S or $M_1$ as discussed above), the chromophore is interacting with its environment in a fashion similar to that in methanol (Loppnow et al., 1989). The solvent methanol removes the counterion from the PSB and solvates the PSB group with hydroxy dipoles (Blatz et al., 1972). The presence of similar chromophore−"solvent" interactions was concluded from the similar ethylenic and single bond stretching frequencies and a similar C═N stretching frequency and $D_2O$ shift for the chromophore in the two environments. However, a more detailed comparison was precluded by the fact that the blue pigment study observed the 9-*cis* isomer and not the 11-*cis* isomer.

A comparison of the sequence of the blue pigment with rhodopsin shows several differences. All blue pigment sequences (Chiu et al., 1994; Hunt et al., 1995; Johnson et al., 1993; Okano et al., 1992; Yokoyama & Yokoyama, 1993) contain serine residues at positions 90 and 295 in proximity

to the Schiff base. The human blue pigment has an additional serine at position 292 (Nathans et al., 1986). This suggests that the hydroxyl-bearing amino acids in the Schiff base vicinity reduce electron delocalization in the chromophore in a fashion similar to that of the solvent methanol. Due to the large uncertainty of the number and orientation of water molecules and protein dipoles in the Schiff base vicinity, the effect of electron repulsion by these dipoles in the Schiff base vicinity was modeled by a retinal-protonated Schiff base with a point charge 2.25 Å from the PSB- proton. The charge distribution along the polyene chain resulting from the INDO calculation is presented in Figure 7A. One observes positively charged carbons close to the PSB terminus and more negatively charged carbons further away from the PSB terminus (and the protein dipoles).

In the other cone pigments, all of the polar residues close to the PSB have been replaced by nonpolar residues (S90G, S292A, and S295A).[5] Figure 7B presents a structural model of the green cone pigment. Several blue pigment hydroxy residues next to the Schiff base group are mutated to nonpolar residues in the green pigment. The retinal polyene chain is color-coded according to the difference in charge distribution resulting from the removal of the negative charge at the Schiff base terminus. Compared to the blue pigment, negative charge density increases in the polyene portion next to the PSB terminus, corresponding to an increase in electron delocalization along the polyene chain. Our calculation predicts that the absorption maximum shifts to longer wavelengths in green pigments along with the increase in delocalization, consistent with the experimentally established correlation between the absorption maximum and electron delocalization.

*Conclusions*. A comparison of the vibrational spectra of several human visual pigments has allowed us to analyze the mechanism of their wavelength regulation. Our conclusions for the tuning mechanism for the three general classes of cone pigments are schematically summarized in Figure 8. In the blue pigment, polar residues in the proximity of the protonated Schiff base reduce electron delocalization along the polyene chain, giving it an environment similar to methanol (Figure 8A). Mutation of several hydroxyl-bearing residues near the Schiff base group (and mutation of a tyrosine residue neighboring the chromophore to the more polarizable tryptophan in the case of group S blue pigments) causes the red shift to the green pigment (Figure 8B). A further red shift is achieved in the red cone pigment by the addition of several hydroxyl-bearing polar groups near the ionone ring end of the retinal chain that interact with the change in the chromophore dipole moment upon excitation (Figure 8C). In rhodopsin, enhanced hydrogen bonding of the Schiff base group, presumably to water, shifts its absorption maximum to lower wavelengths compared to that of the green pigment. It will now be interesting to obtain vibrational spectra of mutants in which the residues responsible for the absorption shifts are replaced to further analyze their role in the wavelength-tuning mechanism of the human visual pigments.

[5] Unlike the blue pigments belonging to the S group (Chiu et al., 1994; Hunt et al., 1995; Okano et al., 1992), the green pigment has a polarizable tryptophan group at position 265 instead of a tyrosine. The mutation W265Y has been shown to blue-shift the absorption maximum of rhodopsin by 10 nm (Nakayama & Khorana, 1991).

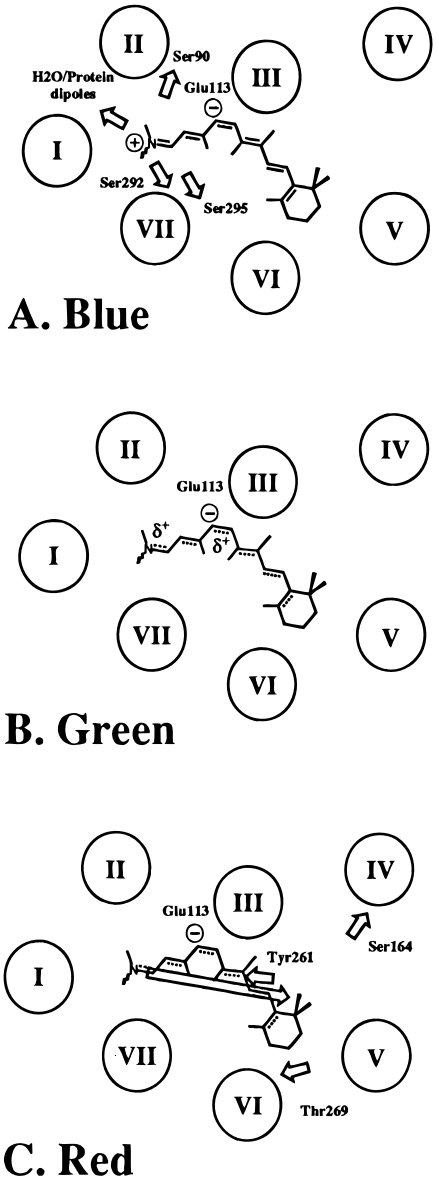


FIGURE 8: Schematic description of the color-tuning mechanism in human cone visual pigments. Protein and water dipoles and the dipole change in retinal upon excitation are depicted by arrows. The $Glu_{113}$ counterion is depicted by a negative charge. The convention used is that a dipole arrow points from − to +.

## ACKNOWLEDGMENT

We thank Steve W. Lin for helpful discussions and Michael J. Tauber and Judy E. Kim for critical reading of the manuscript. We also thank Robert R. Birge for providing us with a copy of the INDO-CI program.

## SUPPORTING INFORMATION AVAILABLE

The CVFF parameters chosen for the 11-*cis*-retinal PSB in the energy minimization, the atomic coordinates and a structural model of the 11-*cis*-retinal PSB and dipoles used in the INDO-CI calculations, and the charge distribution resulting from these calculations (7 pages). Ordering information is given on any current masthead page.

## REFERENCES

Albeck, A., Livnah, N., Gottlieb, H., & Sheves, M. (1992) *J. Am. Chem. Soc. 114*, 2400−2411.

Asenjo, A. B., Rim, J., & Oprian, D. D. (1994) *Neuron 12*, 1131−1138.

Aton, B., Doukas, A. G., Callender, R. H., Becher, B., & Ebrey, T. G. (1977) *Biochemistry 16*, 2995−2999.
Baasov, T., Friedman, N., & Sheves, M. (1987) *Biochemistry 26*, 3210−3217.
Baldwin, J. M. (1993) *EMBO J. 12*, 1693−1703.
Barry, B., & Mathies, R. A. (1987) *Biochemistry 26*, 59−64.
Beppu, Y., & Kakitani, T. (1994) *Photochem. Photobiol. 59*, 660−669.
Birge, R. R., Murray, L. P., Pierce, B. M., Akita, H., Balogh-Nair, V., Findsen, L. A., & Nakanishi, K. (1985) *Proc. Natl. Acad. Sci. U.S.A. 82*, 4117−4121.
Blatz, P. E., & Liebman, P. A. (1973) *Exp. Eye Res. 17*, 573−580.
Blatz, P. E., & Mohler, J. H. (1975) *Biochemistry 14*, 2304−2309.
Blatz, P. E., Mohler, J. H., & Navangul, H. V. (1972) *Biochemistry 11*, 848−855.
Chan, T., Lee, M., & Sakmar, T. P. (1992) *J. Biol. Chem. 267*, 9478−9480.
Chen, J. G., Nakamura, T., Ebrey, T. G., Ok, H., Konno, K., Derguini, F., Nakanishi, K., & Honig, B. (1989) *Biophys. J. 55*, 725−729.
Chiu, M. I., Zack, D. J., Wang, Y., & Nathans, J. (1994) *Genomics 21*, 440−443.
Crescitelli, F. (1982) *Methods Enzymol. 81*, 171−181.
Curry, B. (1983) Ph.D. Thesis, University of California, Berkeley, CA.
Davies, A., Schertler, G. F. X., Gowen, B. E., & Saibil, H. R. (1996) *J. Struct. Biol. 117*, 36−44.
Deng, H., Huang, L., Callender, R., & Ebrey, T. (1994) *Biophys. J. 66*, 1129−1136.
Drikos, G., Rueppel, H., Dietrich, H., & Sperling, W. (1981) *FEBS Lett. 131*, 23−27.
Eyring, G., Curry, B., Broek, A., Lugtenburg, J., & Mathies, R. A. (1982) *Biochemistry 21*, 384−393.
Han, M., & Smith, S. O. (1995) *Biochemistry 34*, 1425−1432.
Han, M., DeDecker, B. S., & Smith, S. O. (1993) *Biophys. J. 65*, 899−906.
Hargrave, P. A., McDowell, J. H., Curtis, D. R., Wang, J. K., Juszczak, E., Fong, S. L., Rao, J. K., & Argos, P. (1983) *Biophys. Struct. Mech. 9*, 235−244.
Honig, B., Greenberg, A. D., Dinur, U., & Ebrey, T. G. (1976) *Biochemistry 15*, 4593−4599.
Huang, L., Deng, H., Weng, G., Koutalos, Y., Ebrey, T., Groesbeek, M., Lugtenburg, J., Tsuda, M., & Callender, R. H. (1996) *Biochemistry 35*, 8504−8510.
Hubbard, A. (1981) Ph.D. Thesis, University of California, Riverside, CA.
Hunt, D. M., Cowing, J. A., Patel, R., Appukuttan, B., Bowmaker, J. K., & Mollon, J. D. (1995) *Genomics 27*, 535−538.
Irving, C. S., Byers, G. W., & Leermakers, P. A. (1970) *Biochemistry 9*, 858−864.
Johnson, R. L., Grant, K. B., Zankel, T. C., Boehm, M. F., Merbs, S. L., Nathans, J., & Nakanishi, K. (1993) *Biochemistry 32*, 208−214.
Kleinschmidt, J., & Harosi, F. I. (1992) *Proc. Natl. Acad. Sci. U.S.A. 89*, 9181−9185.
Kochendoerfer, G. G., Verdegem, P. J. E., van der Hoef, I., Lugtenburg, J., & Mathies, R. A. (1996) *Biochemistry 35*, 16230−16240.
Kojima, D., Imai, H., Okano, T., Fukada, Y., Crescitelli, F., Yoshizawa, T., & Shichida, Y. (1995) *Biochemistry 34*, 1096−1106.
Kropf, A., & Hubbard, R. (1958) *Ann. N.Y. Acad. Sci. 74*, 266−280.
Liang, J., Steinberg, G., Livnah, N., Sheves, M., Ebrey, T. G., & Tsuda, M. (1994) *Biophys. J. 67*, 848−854.
Lin, S. W., Sakmar, T. P., Franke, R. R., Khorana, H. G., & Mathies, R. A. (1992) *Biochemistry 31*, 5105−5111.
Lin, S. W., Imamoto, Y., Fukada, Y., Shichida, Y., Yoshizawa, T., & Mathies, R. A. (1994) *Biochemistry 33*, 2151−2160.
Loppnow, G. R., & Mathies, R. A. (1989) *Rev. Sci. Instrum. 60*, 2628−2630.
Loppnow, G. R., Barry, B. A., & Mathies, R. A. (1989) *Proc. Natl. Acad. Sci. U.S.A. 86*, 1515−1518.
Makino, C. L., Kraft, T. W., Mathies, R. A., Lugtenburg, J., Miley, M. E., van der Steen, R., & Baylor, D. A. (1990) *J. Physiol. (London) 424*, 545−560.
Mathies, R., & Stryer, L. (1976) *Proc. Natl. Acad. Sci. U.S.A. 73*, 2169−2173.
Mathies, R., Oseroff, A. R., & Stryer, L. (1976) *Proc. Natl. Acad. Sci. U.S.A. 73*, 1−5.
Mathies, R. A., Smith, S. O., & Palings, I. (1987) in *Biological Applications of Raman Spectroscopy: Volume 2—Resonance Raman Spectra of Polyenes and Aromatics* (Spiro, T. G., Ed.) pp 59−108, John Wiley & Sons, Inc., New York.
Mendelsohn, R. (1972) *Biochim. Biophys. Acta 290*, 15−21.
Merbs, S. L., & Nathans, J. (1992) *Nature 356*, 433−435.
Nakanishi, K., Balogh-Nair, V., Arnaboldi, M., Tsujimoto, K., & Honig, B. (1980) *J. Am. Chem. Soc. 102*, 7945−7947.
Nakanishi, K., Zhang, H., Lerro, K. A., Takekuma, S., Yamamoto, T., Lien, T. H., Sastry, L., Baek, D., Moquin-Pattey, C., Boehm, M. F., Derguini, F., & Gawinowicz, M. A. (1995) *Biophys. Chem. 56*, 13−22.
Nakayama, T. A., & Khorana, H. G. (1991) *J. Biol. Chem. 266*, 4269−4275.
Nathans, J., & Hogness, D. S. (1984) *Proc. Natl. Acad. Sci. U.S.A. 81*, 4851−4855.
Nathans, J., Thomas, D., & Hogness, D. S. (1986) *Science 232*, 193−202.
Neitz, M., Neitz, J., & Jacobs, G. H. (1991) *Science 252*, 971−974.
Nina, M., Smith, J. C., & Roux, B. (1993) *J. Mol. Struct. 286*, 231−245.
Nina, M., Roux, B., & Smith, J. C. (1995) *Biophys. J. 68*, 25−39.
Okano, T., Kojima, D., Fukada, Y., Shichida, Y., & Yoshizawa, T. (1992) *Proc. Natl. Acad. Sci. U.S.A. 89*, 5932−5936.
Oprian, D. D., Molday, R. S., Kaufman, R. J., & Khorana, H. G. (1987) *Proc. Natl. Acad. Sci. U.S.A. 84*, 8874−8878.
Oprian, D. D., Asenjo, A. B., Lee, N., & Pelletier, S. L. (1991) *Biochemistry 30*, 11367−11372.
Oseroff, A. R., & Callender, R. H. (1974) *Biochemistry 13*, 4243−4248.
Ovchinnikov, Y., Abdulaev, N., Feigina, M., Artamonov, I., Zolotarev, A., Kostina, M., Bogachuk, A., Miroshnikov, A., Martinov, V., & Kudelin, A. (1982) *Bioorg. Khim. 8*, 1011−1014.
Palings, I., Pardoen, J. A., van den Berg, E., Winkel, C., Lugtenburg, J., & Mathies, R. A. (1987) *Biochemistry 26*, 2544−2556.
Palings, I., van den Berg, E. M. M., Lugtenburg, J., & Mathies, R. A. (1989) *Biochemistry 28*, 1498−1507.
Rafferty, C. N., & Shichi, H. (1981) *Photochem. Photobiol. 33*, 229−234.
Rimai, L., Kilponen, R. G., & Gill, D. (1970) *Biochem. Biophys. Res. Commun. 41*, 492−497.
Sawatzki, J., Fischer, R., Scheer, H., & Siebert, F. (1990) *Proc. Natl. Acad. Sci. U.S.A. 87*, 5903−5906.
Schertler, G. F. X., & Hargrave, P. A. (1995) *Proc. Natl. Acad. Sci. U.S.A. 92*, 11578−11582.
Smith, S. O., Pardoen, J. A., Mulder, P. P. J., Curry, B., Lugtenburg, J., & Mathies, R. A. (1983) *Biochemistry 22*, 6141−6148.
Smith, S. O., Marvin, M. J., Bogomolni, R. A., & Mathies, R. A. (1984) *J. Biol. Chem. 259*, 12326−12329.
Tallent, J. R., Hyde, E. W., Findsen, L. A., Fox, G. C., & Birge, R. R. (1992) *J. Am. Chem. Soc. 114*, 1581−1592.
Tanimura, T., Isono, K., & Tsukahara, Y. (1986) *Photochem. Photobiol. 43*, 225−228.
Unger, V. M., & Schertler, G. F. X. (1995) *Biophys. J. 68*, 1776−1786.
Vanquickenborne, L. G. (1991) in *Intermolecular Forces: An Introduction to Modern Methods and Results* (Huyskens, P. L., Luck, W. A. P., & Zeegers-Huyskens, T., Eds.) pp 31−53, Springer-Verlag, Berlin and Heidelberg.
Wald, G., & Brown, P. (1953) *J. Gen. Phys. 37*, 189−200.
Wang, Z., Asenjo, A. B., & Oprian, D. D. (1993) *Biochemistry 32*, 2125−2130.
Yokoyama, R., & Yokoyama, S. (1990) *Proc. Natl. Acad. Sci. U.S.A. 87*, 9315−9318.
Yokoyama, R., & Yokoyama, S. (1993) *FEBS Lett. 334*, 27−31.
Yoshizawa, T. (1972) in *Handbook of Sensory Physiology* (Dartnall, H. J. A., Ed.) pp 148−179, Springer-Verlag, New York.
Yoshizawa, T., & Wald, G. (1967) *Nature 214*, 566−571.

BI970322O